energies

MDPI

Article

Modeling and Experimental Validation of a Volumetric Expander Suitable for Waste Heat Recovery from an Automotive Internal Combustion Engine Using an Organic Rankine Cycle with Ethanol †

José Galindo [1], Vicente Dolz [1,*,‡], Lucía Royo-Pascual [1,‡], Regine Haller [2] and Julien Melis [3]

1 CMT-Motores Térmicos, Polytechnic University of Valencia, 6D Building, Camino de Vera s/n, Valencia 46022, Spain; galindo@mot.upv.es (J.G.); luropas@mot.upv.es (L.R.-P.)
2 Valeo Systèmes Thermiques, 8, rue Louis Lormand, La Verrière 78321, France; regine.haller@valeo.com
3 Exoès S.A.S., 6, avenue de la Grande Lande, Gradignan 33170, France; julien.melis@exoes.com
* Correspondence: vidolrui@mot.upv.es; Tel.: +34-963-877-650
† Part of this work has been presented in 3rd International Seminar on ORC Power Systems, Brussels, Belgium, 12–14 October 2015.
‡ These authors contributed equally to this work.

Academic Editor: Sylvain Quoilin
Received: 19 January 2016; Accepted: 31 March 2016; Published: 9 April 2016

Abstract: Waste heat recovery (WHR) in exhaust gas flow of automotive engines has proved to be a useful path to increase the overall efficiency of internal combustion engines (ICE). Recovery potentials of up to 7% are shown in several works in the literature. However, most of them are theoretical estimations. Some present results from prototypes fed by steady flows generated in an auxiliary gas tank and not with actual engine exhaust gases. This paper deals with the modeling and experimental validation of an organic Rankine cycle (ORC) with a swash-plate expander integrated in a 2 L turbocharged petrol engine using ethanol as working fluid. A global simulation model of the ORC was developed with a maximum difference of 5%, validated with experimental results. Considering the swash-plate as the main limiting factor, an additional specific submodel was implemented to model the physical phenomena in this element. This model allows simulating the fluid dynamic behavior of the swash-plate expander using a 0D model (Amesim). Differences up to 10.5% between tests and model results were found.

Keywords: organic Rankine cycle (ORC); waste heat recovery (WHR); internal combustion engine (ICE); swash-plate; ethanol; modeling; thermal inertia

1. Introduction

In the last years, the interest of improvement in efficiency in internal combustion engine (ICE) has increased, together with the entry into force of ever more stringent anti-pollution regulations. Many of these works are focused on the development of new technologies to recover waste heat from ICEs. Saidur *et al.* [1] propose four different groups to classify these technologies: thermoelectric generators (TEG) [2], organic Rankine cycles (ORC) [3], six-stroke cycle ICE [4] and new developments on turbocharger technology [5,6]. Turbocharging technology for vehicle ICEs has been widely developed in recent decades. In fact, turbochargers are used in practically all Diesel engines found in automotive vehicles. Regarding other available technologies and considering this classification, ORC technology is one of the most promising because of its implementation in the near future engines. ORC technology to recover low-grade heat sources has been wildly developed in geothermal or solar power plants and

also in combined heat and power (CHP) in industrial processes. There are many studies about these facilities, both theoretical and experimental. Some of these theoretical studies describe mathematical models of different ORC facilities for recovery these low temperature heat sources. Table 1 presents a summary of several studies with the main characteristics of the described models.

Table 1. Summary of papers about organic Rankine cycles (ORC) modeling. EES: engineerig equation solver.

References	Model Features	Software	Max. Power	Working Fluid
[7]	ORC with a scroll expander	Amesim	1.5 kW (mechanical)	R245fa
[8]	ORC for CHP with a volumetric expander	Matlab with RefProp	207 kW (output)	R152a, R1234yf, R245fa
[9]	Dynamic ORC model with a turbine	Matlab (Simulink)	8 MW (net power)	Isobutene and R134a
[10]	ORC with a scroll expander	EES	1.8 kW (mechanical)	HCFC-123
[11]	Dynamic ORC model with a turbine	Modelica and Dymola	100 kW	R245fa
[12]	ORC with a scroll expander	Amesim	2.16 kW (mechanical)	R245fa
[13]	Scroll expander	-	260 W (mechanical)	Air and ammonia
[14]	Sliding vane rotary expander	-	2 kW (mechanical)	R236fa
[15]	Reciprocating expander	WAVE Ricardo Software and EES	2.26 kW (output)	Water
[16]	Scroll expander	Matlab with Refprop	2 kW (mechanical)	Several fluids
[17]	Scroll expander	-	1.8 kW (mechanical)	HCFC-123

At present, some studies try to adapt this technology to waste heat recovery (WHR) on vehicle ICEs. WHR technologies seem to assume an essential role in the new regulations of the forthcoming decade. In ICE applications, space and weight restrictions are greater than in industrial installations, which greatly hinders their adaptation. On the other hand, the thermal power available in these engines for WHR is lower than in industrial processes. Therefore, the optimized expander, mass flows and working fluids for heat recovery in ICEs can be different from the options considered in other applications. Typically, the expanders used in industrial ORC facilities are turbines, screws, scrolls or rotary vane expanders [18]. However, ORC design for automotive engines generally presents a reciprocating machine as the optimal solution to convert waste heat energy into mechanical energy, due to the low working fluid flow, low rotational speeds, high expansion ratio values, fluid drop tolerance during its expansion and space restrictions. ORC solutions in automotive applications should be as light and compact as possible, in order to achieve an efficient system with minor modifications to the existing vehicles.

Regarding the working fluids, several authors consider ethanol as a promising fluid due to its good features in the vehicle application temperature range (450–100 °C). Although ethanol is positively evaluated taking into account its environmental, thermo-physical properties and cost, it is classified as a serious hazard by NFPA due to its high flammability. Seher *et al.* [19] concluded that ethanol is one of the most favorable solutions when a reciprocating machine is used as expander. Howell *et al.* [20] selected ethanol as the best working fluid for a successful ORC for a heavy duty (HD) truck. Despite these theoretical studies where ethanol has proven to be the most suitable working fluid for this type of installations, few experimental ORC works with this fluid have been published due to the flammability properties [21]. Therefore, it is necessary to take safety measures to prevent accidents arising from the use of this fluid.

In previous studies, some methodologies to design these cycles have been proposed [22] and applied to define the main characteristics of an ORC facility for WHR in automotive ICEs. This experimental facility has been assembled and tested in order to estimate the viability of this technology. This installation uses a swash-plate reciprocating expander to transform thermal energy into mechanical energy using ethanol as working fluid. The main objective of this paper is to describe and validate a global simulation model of the ORC and a specific submodel of the main limiting factor of the cycle (the swash-plate expander). The proposed models develop in this article using Amesim are consistent due to the slight deviation between experimental and modelled results. The purpose of these models will be: firstly, it should be used to help the understanding of those physical phenomena which are difficult to observe by means experimentation and secondly, in order to estimate

the behavior of the cycle without the need for experimental tests under operating conditions that may cause danger to the installation and/or people.

2. System Layout

As the expander is the most innovative element of these cycles, the description of this system layout has been divided in two parts: in the first part, a general ORC layout is described and in the second one, the expander is characterized.

2.1. Organic Rankine Cycle Layout

In order to perform an experimental evaluation of this system, an ORC test bench was designed and built at CMT-Motores Térmicos in Polytechnic University of Valencia in a research project with the companies Valeo Systèmes Thermiques and Exoès. This facility can be coupled to different types of automotive combustion engines (an automotive diesel engine, a heavy duty diesel engine and an automotive petrol engine). The test bench recovers energy from exhaust gases of a turbocharged 2 L gasoline engine and exchanges thermal energy to the ethanol side (Figure 1).

Figure 1. ORC mock-up.

Figure 2 shows the most relevant components of the ORC mock-up. The running principle is as follows: heat from engine exhaust gases are transferred through the boiler to the working fluid, in this case, ethanol. Then, it is pumped into the high pressure loop and then is evaporated in the boiler and slightly superheated. Thus, working fluid under high temperature and high pressure is generated. After that, the vapour flows into the expander where enthalpy is converted into effective work measured by a torque measuring unit. Low pressure vapour is extracted from the expander and flows to the condenser, reducing its temperature by cooling water and producing condensed ethanol. Therefore, the cycle starts again. The ORC cycle contains as main elements: a boiler, a swash-plate expander, a condenser, a fluid receiver, a subcooler, an expansion vessel and a pump. The condenser is followed by an expansion vessel in order to impose the low pressure in the installation. It is connected to the circuit by means of a three-way valve to the security tank. In closed loop systems with volumetric machines, it is needed tanks in order to ensure the proper availability of working fluid in all operating points and not to have pressure pulses in the inlet of the expander. The ethanol tank is connected with the security tank. The security tank is used to absorb the working fluid in case the level is increased

above the ethanol tank due to pressure pulses. Moreover, this security tank is connected through a manual valve to an additional tank in order to fill the installation. The main elements have been carefully insulated to avoid heat losses to the ambient.

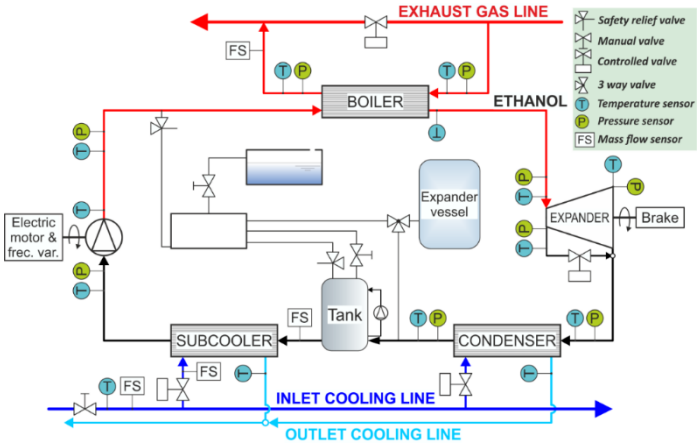

Figure 2. ORC scheme.

The thermodynamic properties of ethanol (pressure and temperature) have been measured upstream and downstream of all components, verifying energy balances and power estimations to ensure the proper operation of all the elements [21]. Table 2 synthesizes the absolute uncertainties of all the sensors installed in the ORC mock-up.

Table 2. Range and accuracy of sensors.

Variable Measured	Type	Range	Accuracy
Exhaust gas pressure	Piezoresistive	0–2 bar	0.05% full scale
Ethanol high pressure loop	Piezoresistive	0–50 bar	0.05% full scale
Ethanol low pressure loop	Piezoresistive	0–5 bar	0.05% full scale
Temperatures	K-type thermocouples (Class 2)	0–1100 °C	±2.5 °C
Ethanol flow meter	Coriolis flow meter	0–2720 kg/h	±0.1%
Water flow meter	Electromagnetic flow sensor	0.3–1 m/s	±0.5% of rate
Expander rotational speed	Optical tachymeter	0–20,000 rpm	±1 rpm
Expander torque meter	Strain gauges	0–200 Nm	0.05% full scale

2.2. Swash-Plate Expander Layout

The expander machine used in this installation is a swash-plate expander (Figure 3). It has been delivered by Exoès. Lower flow rates and higher expansion ratios could be reached in this machine, thus displacement expanders are considered the main technology for recovering waste heat from low temperature sources and low expander power in vehicle applications. The geometrical features of the expander are listed in Table 3.

Table 3. Swash-plate characteristics.

Pistons Number	Bore	Stroke	Maximum Expander Speed
5	40	31	4500
-	mm	mm	rpm

Figure 3. Swash-plate expander delivered by Exoès.

The expander performance has been characterized by the measurement of the indicated diagram (Figure 4). Red and green crosses indicate the intake and exhaust valve closing angle (or volume) respectively. Red and green circles indicate the intake and exhaust valve opening angle (or volume) respectively. The area under the *P-V* curve is the work in J delivered by one piston in each cycle.

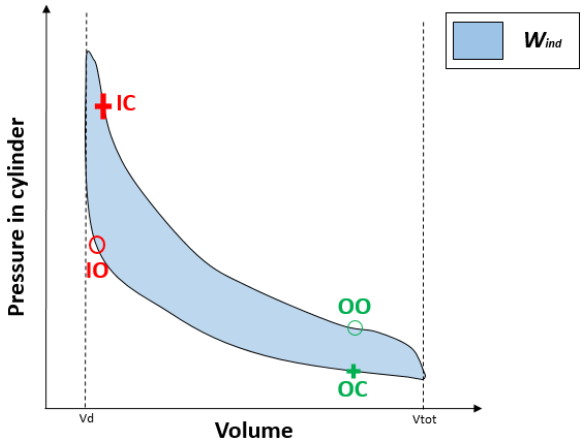

Figure 4. Scheme of *P-V* diagram.

One GU13P piezoelectric pressure sensor (AVL, Stuttgart, Germany) was placed on the chamber of one of the pistons to evaluate the pressure variations (Figure 5). It allows tracking pressure variations during filling and emptying processes. The piezoelectric transducer was connected to a 5015 charge amplifier (Kistler, Ostfildern, Germany). The pressure-volume diagram is used to describe changes of volume and pressure of a system. A swash-plate expander is a positive displacement machine. It works as a two-stroke machine, which means that during one revolution, with a piston movement from the top dead center (TDC) to the bottom dead center (BDC) and back again, one working cycle is completed. The superheated vapour flows through the intake port into the cylinder whose piston is near top dead center. Moving the piston downwards, the vapour expands and leads out by exhaust ports in the cylinder (slits) situated near the bottom dead center. Finally, the upmoving piston closes the exhaust ports and compresses the vapour remained in the cylinder and the cycle starts again. Furthermore, a TDC sensor is used to know the position of the BDC. TDC is an eddy current-Sensor which delivers a signal correlating to the distance between sensor and the swash-plate. The piezoelectric pressure signal has been referenced using low frequency measurement (piezoresistive sensor). A torque meter measured the torque delivered by the expander. In order to measure the expander speed with an ordinary brake, a pulley system was installed in order to increase the expander speed to a brake feasible speed. An exterior oil loop lubricates the swash-plate expander.

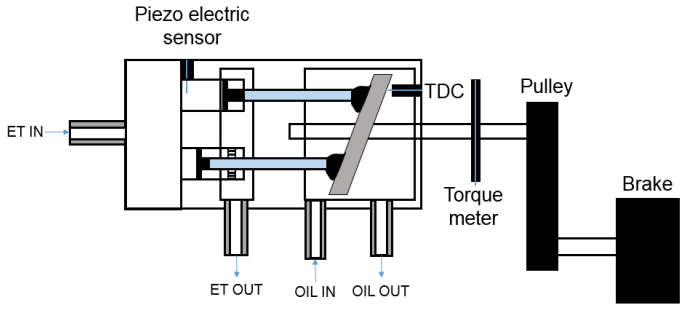

Figure 5. Swash-plate expander scheme. TDC: top dead center.

The analysis of *P-V* diagrams in different conditions can be used to identify the irreversibilities of the expansion machine. All the signals were recorded with a sampling frequency of 50 kHz and processed with program Labview. The engine operating point was fixed until the expander variables were constant (after approximately 15 min). Then, the pressure inside the cylinder was measured during 2 s, which is approximately 50 cycles (depending on the expander speed). After that all the cycles were processed and plotted one over the other cycles.

3. Modelling

The authors have developed a comprehensive model of the ORC using Amesim. Considering the swash-plate expander as the most critical element, one additional specific submodel was implemented to model the physical phenomena inside the piston of the swash-plate expander. The software package provides a 0D model suite to simulate and analyze multi-domain intelligent systems, and to predict their multi-disciplinary performances. This software consists of available object-oriented libraries, where the user should connect them properly and fix the parameters.

3.1. Global Organic Rankine Cycle Model

A simple layout of the ORC consisting of a boiler, a positive displacement pump, a volumetric expander, a fluid receiver, a condenser and an expansion vessel is considered in this model. Figure 6 shows the Amesim model of the cycle based on the ORC installation. A detailed description for the main assumptions in this model are presented in the following subsections.

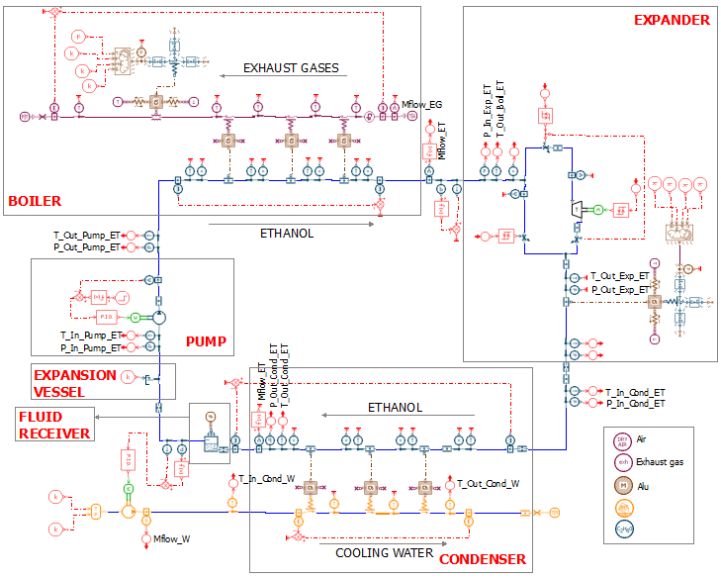

Figure 6. ORC model. Working fluid.

In the modelling of a particular working fluid it is crucial to be able to reproduce both the thermodynamic and transport properties of the working fluid. Amesim provides built-in physical-thermo property data of different fluids. In this case the working fluid is ethanol. Table 4 summarizes the main characteristics of the working fluid.

Table 4. Properties of ethanol.

Property		Ethanol	
Chemical formula		C_2H_6O	
Critical temperature	T_c	240.9	°C
Critical pressure	P_c	61.4	bar
Atmospheric boiling point	T_b	78.3	°C
Ozone depletion potential	ODP	0	-
Global warming potential	GWP	n/a	-
NFPA health hazard	H	2	-
NFPA flammability hazard	F	3	-
Auto ignition temperature	T_{ign}	363	°C

3.1.1. Heat Exchangers

The boiler releases heat from exhaust gases to working fluid, based on plate and fin technology. This is a countercurrent heat exchanger, designed to withstand a maximum pressure of 40 bar. The condenser and the subcooler are plate and fin heat exchangers selected from industrial residential products. The condenser used in the experimental setup is a fin plate exchanger with ethanol as the hot loop and water as the cold loop. It is a stainless steel heat exchanger chosen among industrial residential products. The exchanger was set up in counter current configuration. This is a practical solution to ensure saturated liquid leaves the condenser so that the pump can operate properly. As the operating pressures of this component are relatively low, around 2 bar on both sides, no special attention is required. Plate and fin technology is preferred by the vast majority of the applications due to its compactness and high level of efficiency. A 0D discretization model with different small volumes of both elements (boiler and condenser) is presented by a two-counter flow streams. In the case of the boiler, the exhaust gases and the ethanol represent the hot and cold source respectively. In the case of the condenser, the ethanol and the cooling medium (water) represent the hot and cold source respectively. In each element, the volume has been divided in 3 small volumes, which in global terms exchanges the net thermal power of the global element. The heat exchange process takes into account both convective and conducting (just in longitudinal direction) process. Depending on the process, (boiling or condensation) different correlations implemented in Amesim have been taken into account. Shah correlation [23] and Verein Deutscher Ingenieure (VDI) for horizontal tubes correlation [24] were used for condensation and boiling process respectively.

In order to improve the boiler model and take into account the thermal inertia properly, thermal capacities were adjusted using a transient experimental test. This was performed varying the engine exhaust gases power (and therefore, heat source) from 20 kW to 25 kW. Therefore, the experimental values of exhaust gases mass flow, temperature at the inlet in the exhaust gases side, ethanol mass flow and temperature and pressure at the inlet of the boiler in the ethanol side were used to validate this model. The objective of this validation was to obtain a similar temperature profile at the outlet of the boiler in the ethanol side, considering thermal inertias.

3.1.2. Volumetric Expander

The swash-plate expander is the main element of the ORC system because it has a great impact in the overall system efficiency. The expander model uses three parameters to characterize the performance of the expander, *i.e.*, isentropic efficiency in Equation (1), mechanical efficiency in Equation (2) and volumetric efficiency in Equation (3):

$$\eta_{iso} = \frac{\dot{W}_{ind}}{\dot{W}_{iso}} \quad (1)$$

$$\eta_{mec} = \frac{\dot{W}_{s}}{\dot{W}_{ind}} \quad (2)$$

$$\eta_{vol} = \frac{\dot{m}_{ET}}{\rho_{ET} \times (N_{Exp}/60) \times Disp} \quad (3)$$

$$\dot{W}_{iso} = \dot{m}_{ET} \times \left(h_{in\_Exp\_ET} - h_{out\_Exp\_ET\_iso}\right) \quad (4)$$

$$\dot{W}_{ind} = W_{ind} \times n_{cyl} \times N_{Exp} \times \frac{1}{60} \quad (5)$$

$$\dot{W}_{s} = \tau_{Exp} \times N_{Exp} \times \frac{2 \times \pi}{60} \quad (6)$$

where $\dot{W}_{iso}$, $\dot{W}_{ind}$ and $\dot{W}_{s}$ are isentropic, indicated and shaft power respectively. They have been calculated using Equations (4)–(6) respectively. $\dot{m}_{ET}$ is the mass flow through the expander, $h_{in\_Exp\_ET}$ is the enthalpy at the inlet of the expander (calculated by using temperature and pressure at the inlet), $h_{out\_Exp\_ET_{iso}}$ is the isentropic enthalpy at the outlet of the expander (calculated by using pressure at the outlet and entropy at the inlet). Regarding the expander power, W_{ind} is the indicated work in J, N_{Exp} is the expander speed (rpm) and n_{cyl} the number of cylinders of the expander. Regarding the volumetric efficiency, ρ_{ET} is the density of the ethanol at the inlet of the expander and $Disp$ is the volume displaced by the expander.

No leakages and internal pressure drops have been taken into account in this expander model. Thermal conduction with internal walls of the swash-plate expander is considered to model heat losses to the ambient.

3.1.3. Pump

A fixed displacement pump is used in this model. The mass flow rate is obtained from volumetric efficiency. Mechanical and isentropic efficiency and the swept volume define the enthalpy increase. No correlations have been considered for efficiencies. Instead, some fixed values were specified for the points modelled, *i.e.*, an isentropic efficiency of 80% and a displacement of 5 cm^3.

3.1.4. Pipes and Pressure Drops

Internal piping losses in the system have been taken into account using hydraulic resistances. The transformation process is assumed isenthalpic. Using these elements both enthalpies and mass flows are computed. Pressure drops in the system have been calculated using correlations available in Amesim. The hydraulic diameter and the cross-sectional area were used to model different cross-sectional geometries. The pressure drops are regular and the friction factor depends on the flow regime and the relative roughness of the duct. Depending on the state of the fluid different correlations were applied: In the single phase flow (liquid or vapour) the Churchill [25] correlation was used, while in the two phase flow (TPF) the McAdams *et al.* [26] correlation was implemented. This correlation is used for computing pressure drop inside tubes in vaporization process.

3.1.5. Expansion Vessel

The expansion vessel is modelled using a tank with modulated pressure and constant specific enthalpy. The user must specify the low pressure value with a constant.

3.2. Swash-Plate Specific Model

As shown previously, the volumetric expander tested in this installation is a swash-plate expander. Although in the global ORC model an Amesim submodel of the TPF library was used for modelling the expander using volumetric, isentropic and mechanical efficiencies, the need for an expander physical model has led to the development of a specific model for just the swash-plate expander.

Figure 7 shows the swash-plate expander model. Taking into account the number of pistons in the swash-plate expander, the heat transfer in the compression and expansion process, the swash-plate mechanism and mechanical losses, a swash-plate expander model was developed to simulate the performance of the expander. It was modelled using Amesim and validated with the experimental tests developed in the expander. The comparison between *P-V* diagrams (modelled and tested) was used to estimate the accuracy of the model.

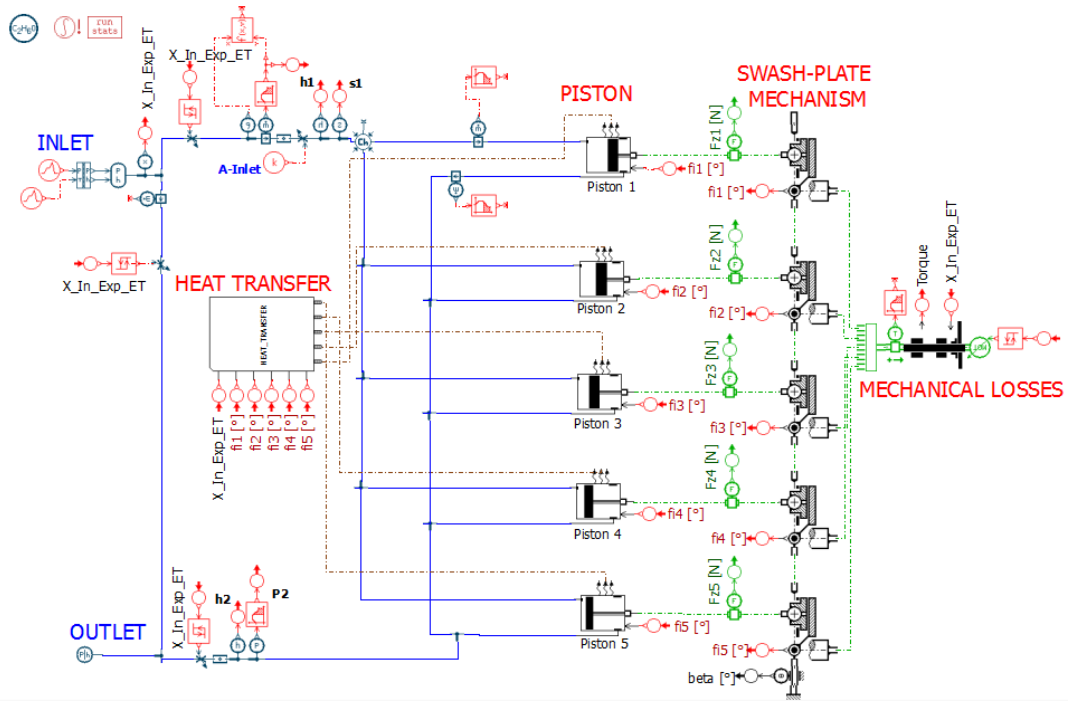

Figure 7. Swash-plate expander model.

Figure 8 shows a zoom of the piston expander modelled in Amesim. The main part of the model consists of a TPF chamber with variable volume and pressure and temperature dynamics. This submodel has been modified from the Amesim original library model to take into account heat transfer during compression and expansion. The filling (intake valve) and emptying (exhaust valve) processes provide the mass and pressure exchanges during the process. The angle signal (obtained from the expander speed) is used in three parts of the model:

- In the heat transfer element: Although the expander was insulated, the expansion and compression do not follow an adiabatic process. The transformation is rather polytropic with a heat exchange between the working fluid and the expander walls due to friction, temperature differences and possible condensation effects in the piston chamber. Therefore, the angle signal was used to consider the angles of compression and expansion and to apply for each process a heat transfer coefficient to model these phenomena.
- In the valves: The angle was considered to take into account the discharge coefficient for the intake and the exhaust valve at each particular angle.

- In the rotary-linear transformer: It was considered to calculate the absolute displacement in Equation (7) and therefore the volume variation in Equation (8) of the piston as a function of the swash-plate angle:

$$X(\Phi) = R_{sw} \times (1 - \cos(\Phi)) \times \tan(\alpha_{sw}) \quad (7)$$

$$V(\Phi) = V_d + \pi \times \frac{B^2}{4} \times X(\Phi) \quad (8)$$

where R_{sw} is the radius of the swash-plate (m), α_{sw} is the swash-plate angle (°), Φ is the angle covered by the piston, V_d is the dead volume (m^3), B is the bore (m), $X(\Phi)$ is the displacement of the piston (m) and $V(\Phi)$ is the volume of the piston (m^3). No leakages effects have been modelled.

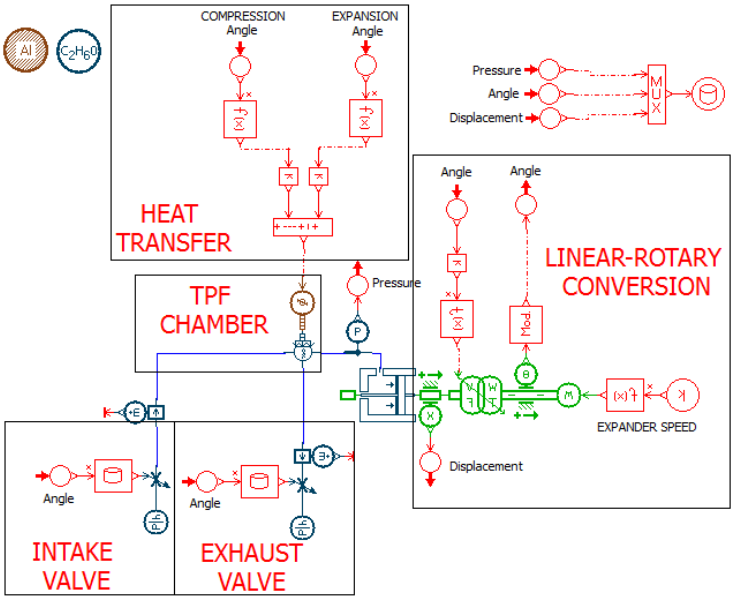

Figure 8. Zoom swash-plate piston expander model.

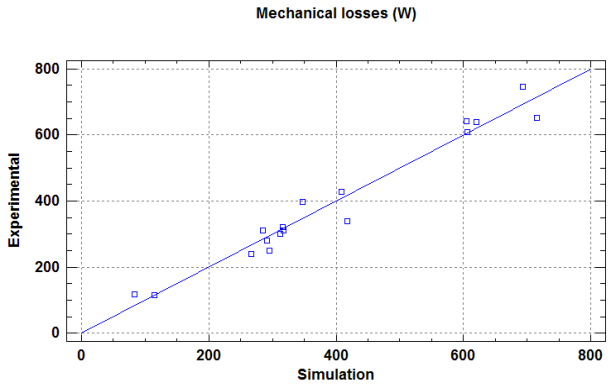

Figure 9. Validation of mechanical losses.

Regarding mechanical losses, they were estimated using experimental values [21]. The following correlation was obtained, taking into account the expansion ratio and the expander speed:

$$Mechanical\ losses\ (W) = 4528.22 - 0.1126 \times N_{Exp} - 285.788 \times \frac{P_{In\_Exp\_ET}}{P_{Out\_Exp\_ET}} \quad (9)$$

where N_{Exp} is the expander speed in rpm and $\frac{P_{In\_Exp\_ET}}{P_{Out\_Exp\_ET}}$ is the expansion ratio through the expander. Figure 9 shows the validation of Equation (9) between estimation and experimental values with a correlation coefficient (R^2) of 96%.

4. Model Validation

4.1. Global Organic Rankine Cycle Model

In order to characterize the ORC system, three points have been tested at different steady working conditions of the ORC system, varying the expander speed (P1: 2000 rpm, P2: 2500 rpm and P3: 3000 rpm). The gasoline engine used in these tests is an inline four-cylinder turbocharged engine (Ford Ecoboost) with a volumetric capacity of 2 L. The engine steady-state operating point has remained constant with a value of 25 kW. The points presented in this study aim to show the recovery features at different expander operating points [21]. In these tests, the system has been controlled commanding three parameters: the speed of the pump, in order to control the mass flow of ethanol flowing through the installation, the balloon pressure of the expansion vessel, in order to control the outlet pressure of the expander, and the expander speed, in order to control the high pressure at the inlet of the expander.

Table 5 shows the inputs of the ORC model. For each point (P1, P2 and P3), the mass flow of the expander, the pressure at the inlet of the pump, the expander speed, the temperature at the inlet of the boiler inthe EG side, the pressure at the boiler in the EG side, the mass flow of the exhaust gases and the temperature at the inlet of the condenser in the water side were fixed.

Table 5. Inputs of the ORC model.

Variable	P1	P2	P3	Units
$\dot{m}_{ET}$	73.85	75.99	74.79	kg/h
$P_{\_in\_PP\_ET}$	1.571	1.899	1.589	bar
N_{Exp}	2001	2502	3003	rpm
$T_{\_in\_B\_EG}$	749.5	740	749	°C
$P_{\_out\_B\_EG}$	1.018	1.024	1.018	bar
$\dot{m}_{EG}$	154.98	159.47	155.25	kg/h
$T_{\_in\_C\_W}$	48.5	49	48	°C

Table 6 shows the volumetric, the isentropic, the mechanical efficiency (calculated using Equations (1)–(3)) and the global efficiency of the expander (defined by the isentropic efficiency times the mechanical efficiency). They have been fixed in the model.

Table 6. Experimental efficiencies of the swash-plate expander.

Variable	P1	P2	P3	Units
$\dot{W}_{ind}$	1739	2007	1874	W
$\dot{W}_{mec}$	1649	1543	1531	W
$\dot{W}_{iso}$	3431	3413	3338	W
η_{vol}	19.37%	17.21%	14.54%	-
η_{iso}	50.68%	58.81%	56.14%	-
η_{mec}	94.81%	76.90%	81.72%	-
η_{glob}	48.05%	45.22%	45.88%	-

Table 7 presents the outputs of the model for the three points tested. For each point three columns are presented, the first one, called "P_i E", corresponds to the experimental values, the second one, called "P_i M", corresponds to the modelled values and the last one, called "Dif.", corresponds to the

absolute difference experimental-modelled. Temperatures are given in °C, pressures in bar, and torque in Nm.

Table 7. Outputs of the ORC model.

Variable	P1 E	P1 M	Difference	P2 E	P2 M	Dif.	P3 E	P3 M	Dif.	Units
$T_{\_out\_PP\_ET}$	47.5	46.5	0.31%	47	46	0.25%	48.5	46	0.70%	°C
$T_{\_out\_B\_ET}$	210	209	0.33%	215	199	3.28%	208	201	1.44%	°C
$T_{\_out\_Exp\_ET}$	105	116	3.04%	109	107	0.50%	111	110	0.30%	°C
$T_{\_in\_C\_ET}$	104	102.5	0.33%	103	99	1.16%	102	97	1.37%	°C
$T_{\_out\_C\_ET}$	48	48.5	0.10%	48	48.5	0.17%	48	48.5	0.22%	°C
$T_{\_in\_PP\_ET}$	46.5	46	0.28%	46.5	46	0.23%	47.5	46	0.53%	°C
$T_{\_out\_C\_W}$	74	71	0.71%	67	69	0.52%	73	71.5	0.38%	°C
$P_{\_out\_PP\_ET}$	34.26	34.26	0.01%	31.01	31.48	1.51%	31.77	31.16	1.92%	bar
$P_{\_in\_Exp\_ET}$	28.65	29.57	3.20%	27.00	26.53	1.74%	26.01	26.36	1.33%	bar
$P_{\_in\_C\_ET}$	1.89	1.89	0.20%	2.01	2.10	4.48%	1.90	1.88	0.95%	bar
τ_{Exp}	7.81	7.98	2.18%	5.86	5.59	4.47%	4.87	4.96	1.85%	Nm

Figures 10–13 show the validation of this model in each particular point. As regards temperatures, the maximum deviation corresponds to the temperature at the inlet of the expander in the 2500 rpm, with a value of 3.28% (Figure 11). The remainder temperatures of the cycle are modelled with a difference lower than 3%. Regarding pressures, the maximum deviation corresponds to the pressure at the inlet of the condenser in the 2500 rpm, with a value of 4.48% (Figure 11). The remainder pressures of the system are calculated with a difference of 3%. The last parameter is the torque delivered by the expander (Figure 13), in which the maximum deviation is approximately 4%, which are in order of magnitude of the measurement errors.

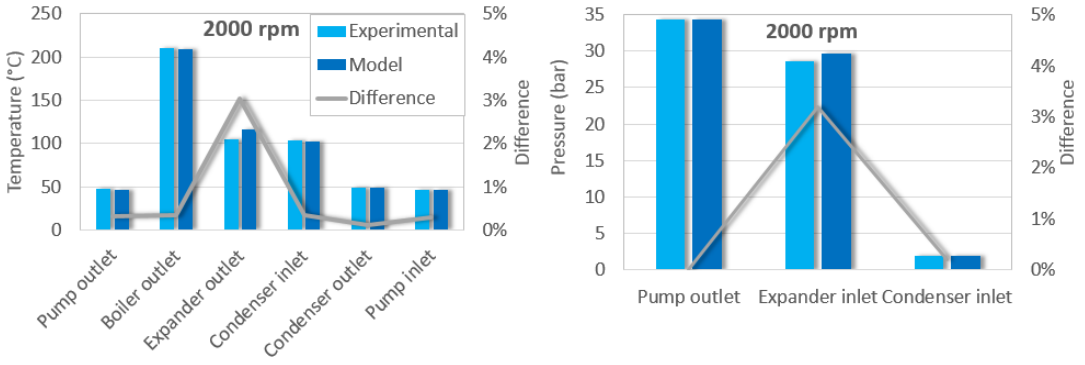

Figure 10. Validation of 2000 rpm.

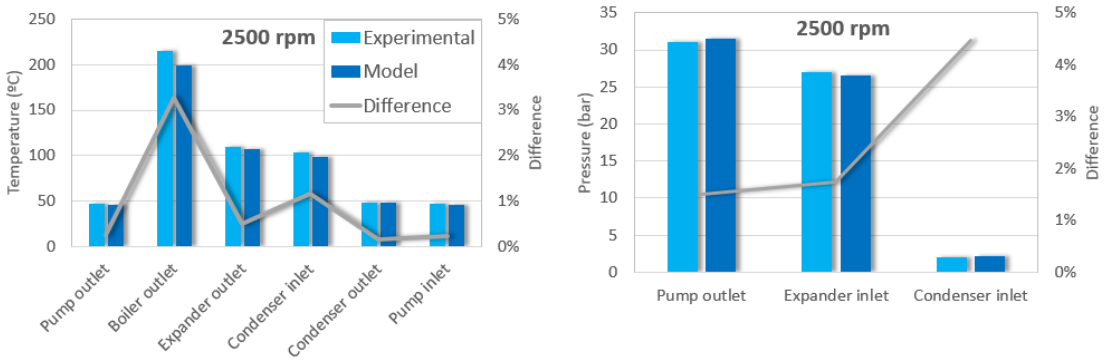

Figure 11. Validation of 2500 rpm.

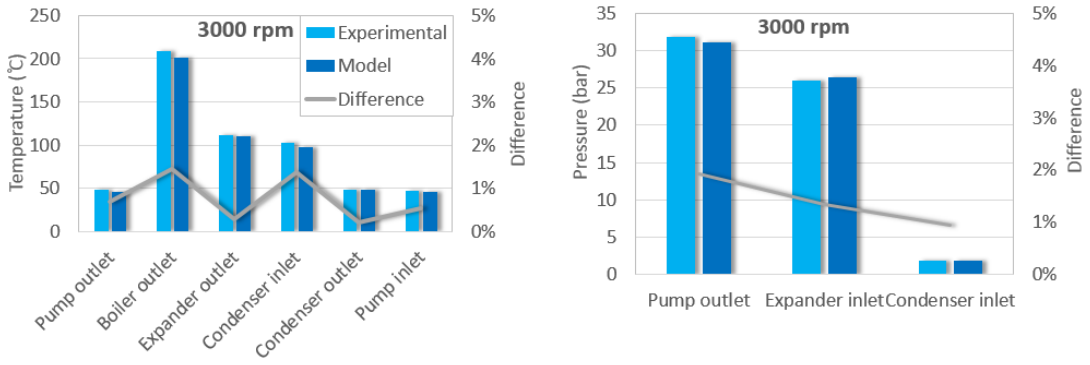

Figure 12. Validation of 3000 rpm.

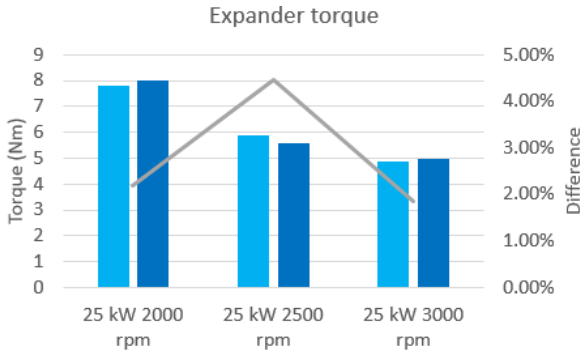

Figure 13. Validation of torque.

Regarding the thermal inertias of the boiler, the modelled and experimental curves of temperature variation outside the boiler in the ethanol side as a function of time were compared. As shown in Figure 14, the temperature at the outlet of the boiler in the ethanol side considering a mass of 3 kg (1 kg in each node) seem to fit quite well with the experimental value. Temperatures differences lower than 4% were found comparing model and experimental values.

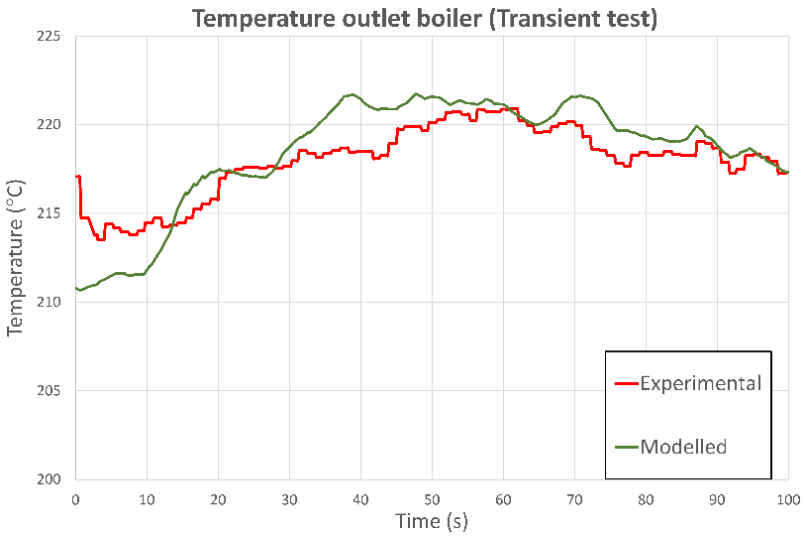

Figure 14. Validation of temperature in the boiler.

4.2. Swash-Plate Specific Model

The modelled and experimental curves of the pressure variation inside the expander chamber as a function of volume are compared for the three points tested in previous sections (3000 rpm, 2500 rpm and 2000 rpm) in Figures 15–17.

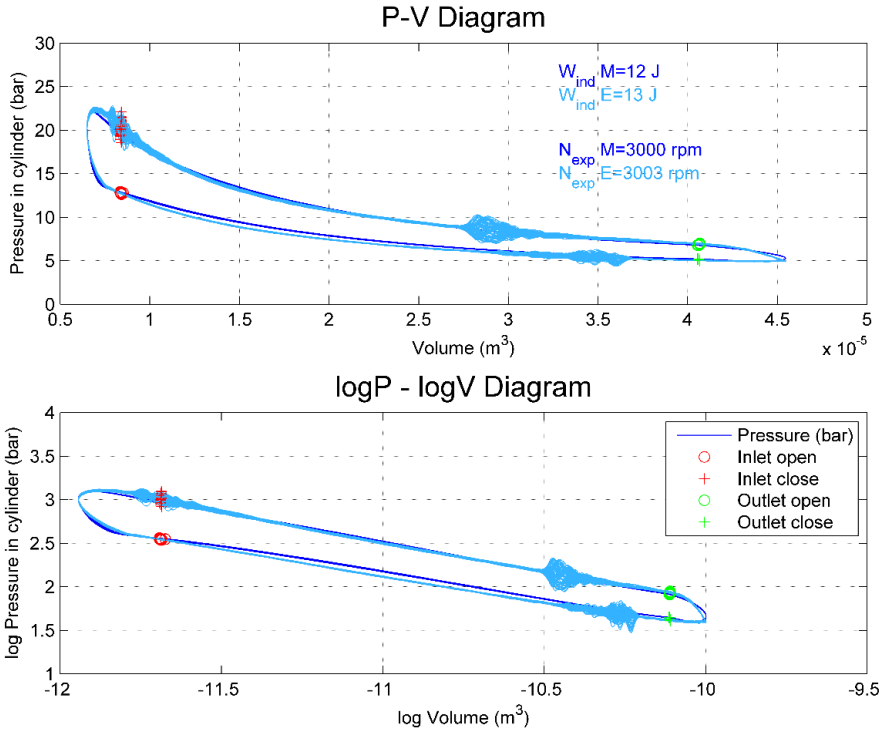

Figure 15. *P-V* Diagram 3000 rpm.

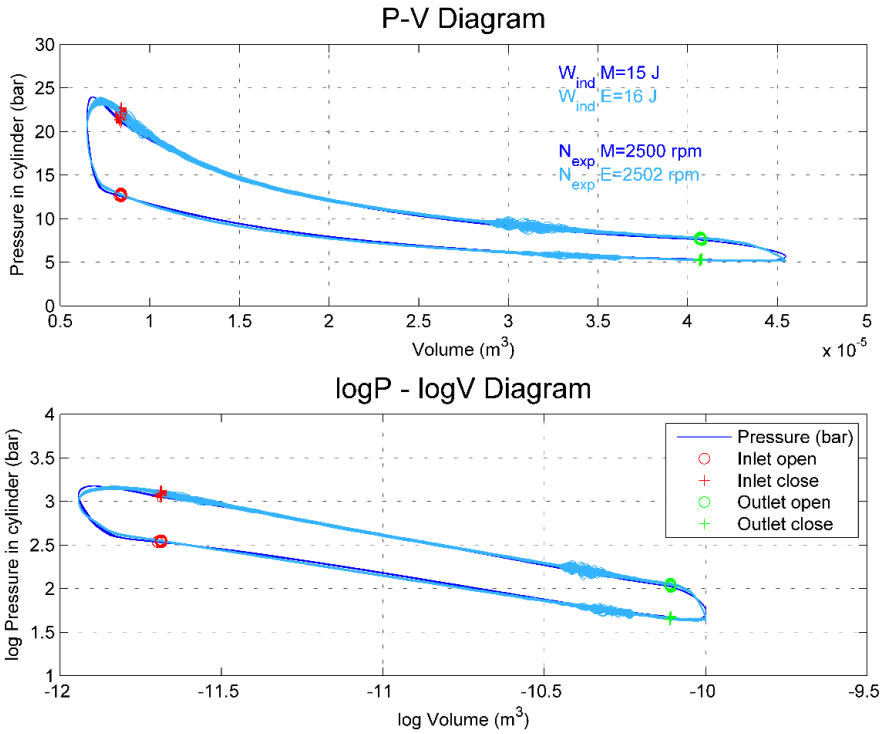

Figure 16. *P-V* Diagram 2500 rpm.

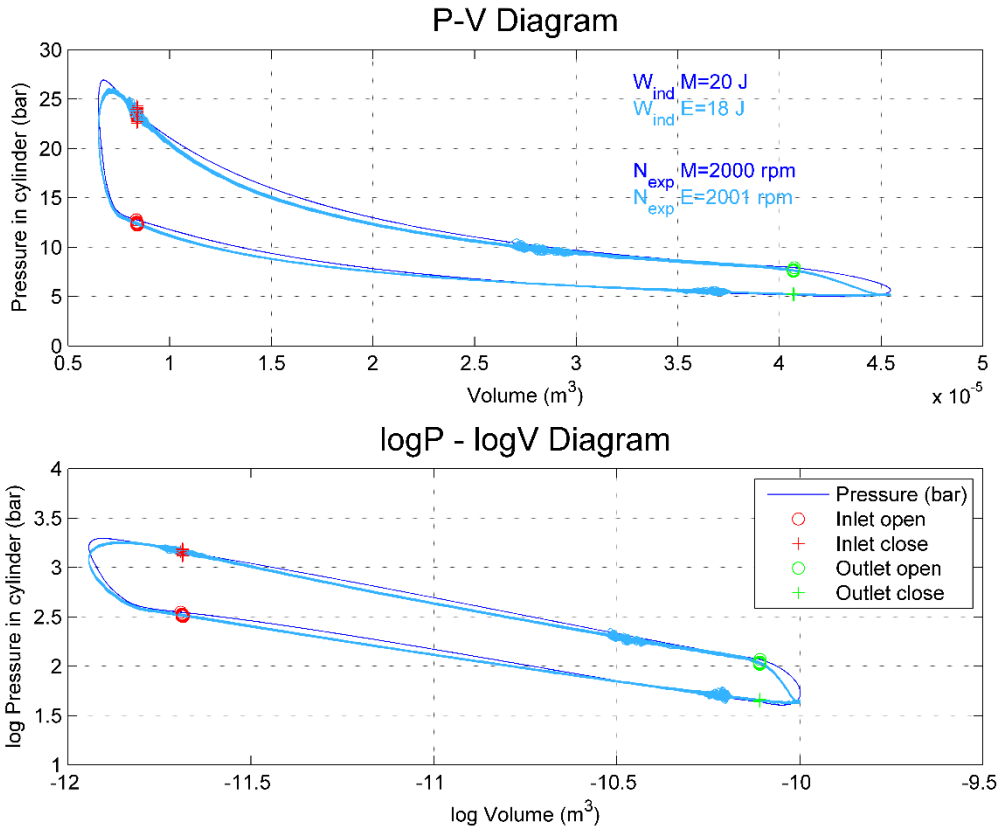

Figure 17. *P-V* Diagram 2000 rpm.

It was found a quite good agreement between experimental and modelled results in terms of indicated work delivered by the expander. In the right corner of these diagrams both the indicated work and the expander speed were presented. Differences up to 10.5% could be found in these models due to pressure drop in the valves and effects of pulsating flow, which is not modelled in Amesim with the TPF library.

Table 8. Results of the swash-plate model.

Variable	P1	P2	P3	Units	I/O
$P_{in\_Exp\_ET}$	28.65	27.00	26.01	bar	Input
N_{Exp}	2001	2502	3003	rpm	Input
W_{ind_E}	18	16	13	J	-
W_{ind_M}	20	15	12	J	Output
$\dot{W}_{ind\_E}$	1739	2007	1874	W	-
$\dot{W}_{ind\_M}$	1857	1877	1678	W	Output
Dif. Power (%)	6.79%	6.48%	10.46%	-	-

Table 8 summarizes the results of the models. The inputs of the model were obtained from pressure measurements at the inlet of the expander and expander speed. In order to take into account differences between heat transferred in the three points, the coefficients of compression and expansion were modified. In this model the higher the expander speed is, the higher heat transfer rate should be imposed in the model. Table 8 also shows the results of the indicated power in W. The maximum power deviation between experimental and modelled results corresponds to 10% in the point of 3000 rpm, which is considered acceptable to predict flow behavior. Although in this point the *P-V* diagram fits better than the others, the expander speed modifies this effect due to the computation of the indicated

power using Equation (5). Besides, the model predicts properly the filling and emptying processes, as it can be seen in Figures 15–17.

5. Conclusions

The presented work describes and analyzes some models based on an experimental ORC installation installed in a turbocharged 2.0 L gasoline engine to recover waste heat in exhaust gases. These models correspond on the one hand to the global ORC cycle and on the other hand to a specific submodel of the swash-plate expander. The comparison of performance parameters have been made in three points by means of changing the inputs and obtaining the outputs of the model. The results are summarized in the following points:

(1) An ORC model was developed using the software Amesim. This model allows to simulate the main parameters measured in the cycle. Comparing the three steady operating points, a maximum deviation of 4% regarding pressures and temperatures and a value of 5% regarding torque was attained.

(2) A swash-plate expander model was presented using the software Amesim. This model represents the fluid dynamic behavior of the swash-plate using discharge coefficients, displacement laws, heat transfer coefficients and mechanical losses. The *P-V* diagram was measured by a piezoelectric pressure sensor and was compared to the expander model one. Maximum deviation of 10% in indicated power was achieved at point of 3000 rpm.

Acknowledgments: This work is part of a research project called "Evaluation of bottoming cycles in ICEs to recover waste heat energies" funded by a National Project of the Spanish Government with reference TRA2013-46408-R. The authors thank also to Raul Luján and Rafael Carrascosa for their contribution in the testing process. Authors want to acknowledge the "Apoyo para la investigación y Desarrollo (PAID)" grant for doctoral studies (FPI S2 2015 1067).

Author Contributions: Lucía Royo-Pascual conceived and performed the model; Vicente Dolz and José Galindo reviewed the model and analyzed the data; Regine Haller and Julien Melis contributed with analysis and experimental tools.

Conflicts of Interest: The authors declare no conflict of interest.

Abbreviations

BDC	Bottom dead center
ICE	Internal combustion engine
CHP	Combined heat and power
WHR	Waste heat recovery
NFPA	National fire protection association
HD	Heavy duty
E	Experimental
M	Modelled
ORC	Organic Rankine cycle
P-V	Pressure volume
TDC	Top dead center
TPF	Two phase flow
ODP	Ozone depletion potential
GWP	Global warming potential

Nomenclature

η	Efficiency
$\dot{W}$	Power (kW)
W	Work (J)
N	Expander speed (rpm)
$\dot{m}$	Mass flow (kg/h)
P	Pressure (bar)
T	Temperature (°C)
ρ	Density (kg/m^3)
n	Number of cylinders
Pi	State point i
τ	Torque (Nm)
$Disp$	Displacement single cylinder (m^3)
Vd	Dead volume (m^3)
B	Cylinder bore (m)
$Rswash$	Radius of the swash-plate (m)
X	Displacement covered by the piston (m)
V	Volume covered by the piston (m)

Subscript

ET	Ethanol
W	Water
EG	Exhaust gases
PP	Pump
Exp	Expander
C	Condenser
B	Boiler
In	Inlet
Out	Outlet
Iso	Isentropic
Ind	Indicated
S	Shaft
Vol	Volumetric
Mec	Mechanical
cyl	Cylinder

References

1. Saidur, R.; Rezaei, M.; Muzammil, W.K.; Hassan, M.H.; Paria, S.; Hasanuzzaman, M. Technologies to recover exhaust heat from internal combustion engines. *Renew. Sustain. Energy Rev.* **2012**, *16*, 5649–5659. [CrossRef]
2. Yang, J. Potential Applications of Thermoelectric Waste Heat Recovery in the Automotive Industry. In Proceedings of the 24th International Conference on Thermoelectric 2005 ICT, Clemson, SC, USA, 19–23 June 2005; pp. 170–174.
3. Apostol, V.; Pop, H.; Dobrovicescu, A.; Prisecaru, T.; Alexandru, A.; Prisecaru, M. Thermodynamic analysis of ORC configurations used for WHR from a turbocharged diesel engine. *Procedia Eng.* **2015**, *100*, 549–558. [CrossRef]
4. Conklin, J.C.; Szybist, J.P. A highly efficient six-stroke internal combustion engine cycle with water injection for in-cylinder exhaust heat recovery. *Energy* **2010**, *35*, 1658–1664. [CrossRef]

5. Dolz, V.; Novella, R.; García, A.; Sánchez, J. HD Diesel engine equipped with a bottoming Rankine cycle as a waste heat recovery system. Part 1: Study and analysis of the waste heat energy. *Appl. Therm. Eng.* **2012**, *36*, 269–278. [CrossRef]
6. Serrano, J.R.; Dolz, V.; Novella, R.; García, A. HD Diesel engine equipped with a bottoming Rankine cycle as a waste heat recovery system. Part 2: Evaluation of alternative solutions. *Appl. Therm. Eng.* **2012**, *36*, 279–287. [CrossRef]
7. Bracco, R.; Clemente, S.; Micheli, D.; Reini, M. Experimental tests and modelization of a domestic-scale ORC (Organic Rankine Cycle). *Energy* **2013**, *58*, 107–116. [CrossRef]
8. Lecompte, S.; Huisseune, H.; Van den Broek, M.; De Schampheleire, S.; De Paepe, M. Part load based thermo-economic optimization of the Organic Rankine Cycle (ORC) applied to a combined heat and power (CHP) system. *Appl. Energy* **2013**, *111*, 871–881. [CrossRef]
9. Manente, G.; Toffolo, A.; Lazzaretto, A.; Paci, M. An organic Rankine cycle off-design model for the search of the optimal control strategy. *Energy* **2013**, *58*, 97–106. [CrossRef]
10. Quoilin, S.; Lemort, V.; Lebrun, J. Experimental study and modeling of an Organic Rankine Cycle using scroll expander. *Appl. Energy* **2010**, *87*, 1260–1268. [CrossRef]
11. Wei, D.; Lu, X.; Lu, Z.; Gu, J. Dynamic modeling and simulation of an Organic Rankine Cycle (ORC) system for waste heat recovery. *Appl. Therm. Eng.* **2008**, *28*, 1216–1224. [CrossRef]
12. Ziviani, D.; Beyene, A.; Venturini, M. Advances and challenges in ORC systems modeling for low grade thermal energy recovery. *Appl. Energy* **2014**, *121*, 79–95. [CrossRef]
13. Mendoza, L.C.; Navarro-Esbrí, J.; Bruno, J.C.; Lemort, V.; Coronas, A. Characterization and modeling of a scroll expander with air and ammonia as working fluid. *Appl. Therm. Eng.* **2014**, *70*, 630–640. [CrossRef]
14. Cipollone, R.; Bianchi, G.; Di Battista, D.; Contaldi, G.; Murgia, S. Mechanical energy recovery from low grade thermal energy sources. *Energy Procedia* **2014**, *45*, 121–130. [CrossRef]
15. Ferrara, G.; Manfrida, G.; Pescioni, A. Model of a small steam engine for renewable domestic CHP (combined heat and power) system. *Energy* **2013**, *58*, 78–85. [CrossRef]
16. Giuffrida, A. Modelling the performance of a scroll expander for small organic Rankine cycles when changing the working fluid. *Appl. Therm. Eng.* **2014**, *70*, 1040–1049. [CrossRef]
17. Lemort, V.; Quoilin, S.; Cuevas, C.; Lebrun, J. Testing and modeling a scroll expander integrated into an Organic Rankine Cycle. *Appl. Therm. Eng.* **2009**, *29*, 3094–3102. [CrossRef]
18. Qiu, G.; Liu, H.; Riffat, S. Expanders for micro-CHP systems with organic Rankine cycle. *Appl. Therm. Eng.* **2011**, *31*, 3301–3307. [CrossRef]
19. Seher, D.; Lengenfelder, T.; Gerhardt, J.; Eisenmenger, N.; Hackner, M.; Krinn, I. Waste Heat Recovery for Commercial Vehicles with a Rankine Process. In Proceedings of the 21st Aachen Colloquium Automobile and Engine Technology, Aachen, Germany, 11 October 2012; pp. 7–9.
20. Howell, T.; Gibble, J. Development of an ORC System to Improve HD Truck Fuel Efficiency. In Proceedings of Deer Conference, Deer, MA, USA, 5 October 2011; pp. 1–21.
21. Galindo, J.; Ruiz, S.; Dolz, V.; Royo-Pascual, L.; Haller, R.; Nicolas, B.; Glavatskaya, Y. Experimental and thermodynamic analysis of a bottoming Organic Rankine Cycle (ORC) of gasoline engine using swash-plate expander. *Energy Convers. Manag.* **2015**, *103*, 519–532. [CrossRef]
22. Macián, V.; Serrano, J.R.; Dolz, V.; Sánchez, J. Methodology to design a bottoming Rankine cycle, as a waste energy recovering system in vehicles. Study in a HDD engine. *Appl. Energy* **2013**, *104*, 758–771. [CrossRef]
23. Shah, M.M. A general correlation for heat transfer during film condensation inside pipes. *Int. J. Heat Mass Transf.* **1979**, *22*, 547–556. [CrossRef]
24. Steiner, D.; Taborek, J. Flow boiling heat transfer in vertical tubes correlated by an asymptotic model. *Heat Transf. Eng.* **1992**, *13*, 43–69. [CrossRef]
25. Churchill, S.W. Friction-factor equation spans all fluid flow regimes. *Chem. Eng.* **1977**, *84*, 91–92.
26. McAdams, W.H.; Woods, W.K.; Heroman, L.C. Vaporization inside horizontal tubes -II- Benzene-oil mixtures. *Trans. ASME* **1942**, *64*, 193–200.